VERTICAL FACING PANEL-JOINT GAP ANALYSIS FOR STEEL-REINFORCED SOIL WALLS

I.P. Damians[1]
R.J. Bathurst[2] (corresponding author)
A. Lloret[3]
A. Josa[4]

[1] Ph.D. Candidate, Department of Geotechnical Engineering and Geo-Sciences (ETCG) and Institute for Sustainability (IS.UPC). Universitat Politècnica de Catalunya-BarcelonaTech (UPC), Spain; Phone: (+34) 93 401 1695, Fax: (+34) 93 401 7251, E-mail: ivan.puig@upc.edu

[2] Professor, GeoEngineering Centre at Queen's-RMC, Civil Engineering Department, 13 General Crerar, Sawyer Building, Room 3417 Royal Military College of Canada Kingston, Ontario K7K 7B4, Canada; Phone: (+1) 613 541 6000 ext, 6479, Fax: (+1) 613 541 6218, E-mail: bathurst-r@rmc.ca

[3] Professor, Department of Geotechnical Engineering and Geo-Sciences (ETCG). Universitat Politècnica de Catalunya-BarcelonaTech (UPC), Spain; Phone: (+34) 93 401 6870, Fax: (+34) 93 401 7251, E-mail: antonio.lloret@upc.edu

[4] Professor, Department of Geotechnical Engineering and Geo-Sciences (ETCG) and Institute for Sustainability (IS.UPC). Universitat Politècnica de Catalunya-BarcelonaTech (UPC), Spain; Phone: (+34) 93 401 7260, Fax: (+34) 93 401 7251, E-mail: alejandro.josa@upc.edu

Abstract

This paper reports the results of a numerical parametric study focused on the prediction of vertical load distribution and vertical gap compression between precast concrete facing panel units in steel reinforced soil walls ranging in height from 6 m to 24 m. The vertical compression is accommodated by polymeric bearing pads placed at the horizontal joints between panels during construction. The paper demonstrates how gap compression and magnitude of vertical load transmitted between horizontal joints are influenced by joint location along the height of the wall, joint compressibility, and backfill and foundation soil stiffness. The summary plots in this study can be used to estimate the number and type (stiffness) of the bearing pads to ensure a target minimum gap thickness at the end of construction, demonstrate the relative influence of wall height and different material component properties on vertical load levels and gap compression, or used as a benchmark to test numerical models used for project-specific design. The paper also demonstrates that while the load factor (ratio of vertical load at a horizontal joint to weight of panels above the joint) and joint compression are relatively insensitive to foundation stiffness, the total settlement at the top of the wall facing is very sensitive to foundation stiffness. The paper examines the quantitative consequences of using a simple linear compressive stress-strain model for the bearing pads versus a multi-linear model which is better able to capture the response of bearing pads taken to greater compression. The study demonstrates that qualitative trends in vertical load factor are preserved when a more advanced stress-dependent stiffness soil hardening model is used for the backfill soil compared to the simpler linear-elastic Mohr-Coulomb model. While there are differences in vertical loads and gap compression using both soil models for the backfill, the differences are small and not of practical concern.

CE Database subject headings: Retaining structures; Reinforcing steel; Panels; Finite element method.

Author keywords: Soil retaining walls; Steel reinforcement; Vertical loads; Facing panels; Bearing pads; Finite element modeling.

Introduction

Steel reinforced soil walls constructed with steel strips, bar mats or steel ladders that are attached to steel-reinforced concrete panels are a mature technology. The design focus in guidance documents used by geotechnical engineers is most often on the internal and external stability of the gravity mass formed by the facing panels and reinforced soil zone (e.g., **AASHTO 2014**). However, the facing column is an important structural component of these systems. It must be designed to carry vertical loads that are greater than the self-weight of the panels. **Damians et al. (2013)** collected data from instrumented steel reinforced soil walls and found that the ratio of measured vertical load to panel self-weight (load factor) ranged from about 2 to 5. These additional vertical loads are the result of downdrag forces generated by backfill soil-panel interface shear due to relative settlement of the backfill plus parasitic downward loads generated at the connections between the steel soil reinforcement elements and the back of the facing (**Figure 1**). The relative stiffness of the backfill soil and the horizontal joint (bearing pad) stiffness will influence the magnitude of downdrag loads acting at the wall face and connections. If vertical downdrag loads are excessive and/or joint stiffness is too low, then the panels can come into contact leading to spalling and/or failure of the concrete panels. Documented examples of these types of failures are given in the paper by **Damians et al. (2013**). While panel facing damage due to loss of gap space is visually detectable it does not typically threaten the overall stability of the structure. For this reason when it does occur, it is ranked as moderately significant based on a post-construction inspection and performance assessment protocol developed in the USA (**Gerber 2012**) even though wall appearance may be unsatisfactory to the observer.

In an earlier related study, the writers carried out a numerical parametric analysis to investigate the influence of joint compressibility, reinforced soil stiffness and foundation stiffness on vertical panel loads and gap compression using the case of a single wall of height H = 16.7 m (**Damians et al. 2013**). The parameters varied were joint axial stiffness (compressibility due to the number and type (stiffness) of the bearing pads), backfill soil and foundation stiffness. The numerical modelling was carried out using the program **PLAXIS (2008)** together with simple linear elastic-plastic constitutive models for the component materials. The same finite element

modeling package with the same constitutive models for the component materials and interfaces has been used to satisfactorily reproduce the behavior of an instrumented 16.7 m-high steel strip reinforced soil wall (**Damians et al. 2015**). Lessons learned regarding the use of program PLAXIS to model reinforced soil walls with discontinuous reinforcement layers can be found in the papers by **Yu et al. (2015a, b)**.

The numerical simulation results reported by **Damians et al. (2013)** also confirmed physical measurements mentioned earlier that the magnitude of the vertical load between panels was always greater than the panel self-weight above the joint. The ratio of vertical load to panel self-weight (load factor) ranged from about 2 to 7 depending on the relative joint stiffness and the relative stiffness of the backfill soil and the foundation soil in their numerical simulations. The numerical simulation results for H = 16.7 m and interface friction coefficient R = 0.3 were shown to be consistent with computed load factors from field measurements in the range of about 2 to 5 for joint stiffness values of about 0.1 to 1.1 MPa/m.

The paper by **Damians et al. (2013)** is an important start to identify issues related to joint compressibility and design, and to demonstrate the influence of wall joint compressibility and stiffness of the backfill soil and foundation on vertical loads developed in the concrete panel facing units of steel reinforced soil walls. However, this earlier work was limited to a single wall height and simple constitutive models and assumptions for the component materials (e.g. linear elastic models with Mohr Columb failure criterion for the soil and linear elastic reinforcement). Furthermore, numerical outcomes were restricted to the bottom (most critical) joint without reporting the behavior of the horizontal joints along the entire height of the wall. Questions remain regarding possible differences in the quantitative results and qualitative trends reported in this earlier study with respect to other wall heights. To answer these questions, numerical simulation of walls with height H = 6, 12, 18 and 24 m were carried out and their performance summarized. In addition, the influence of constitutive model type for the backfill soil and load-compression behavior of the bearing pads is also explored in more detail.

Bearing Pads

A detailed explanation of the role of the polymeric bearing pads that are placed at the horizontal joints between the concrete panels in steel reinforced soil walls can be found in the paper by **Damians et al. (2013)**. A brief summary of the important points is repeated here for completeness.

The primary functions of bearing pads are to act as spacers to: 1) transfer vertical load between the concrete facing panels; 2) accommodate possible differential settlements between the backfill and the facing; and, 3) prevent contact between the panels. In the USA a minimum gap of thickness of 12 mm is recommended after the wall is constructed (**Berg et al. 2009**). In the UK the recommended minimum gap thickness is 1/150 of the panel height (**BSI BS8006 2010**). Hence, for a panel height of 1.5 m (the case in this study) the minimum gap thickness at end of construction is 10 mm. Clearly, to meet these performance criteria the number of bearing pads (typically a minimum of two), stiffness (compressibility) and thickness of the bearing pads (typically 20 – 25 mm) are of primary importance. The most common bearing pad materials are EPDM (ethylene propylene diene monomer) and HDPE (high density polyethylene). Measurements of gap closure have been reported in the literature. **Finlay (1978)** reported a maximum closure of 10 mm for a 6.3 m-high section of wall and **Choufani et al. (2011)** reported 20 mm of gap closure for a 20 m-high wall constructed with 25 mm-thick bearing pads.

Numerical Model Details

General

The 2D finite element method (FEM) program **PLAXIS (2008)** was used to carry out the numerical simulations in this study. **Figure 2** shows the finite element mesh (15-node triangle elements) and geometry adopted in the analyses. Four wall heights were considered corresponding to H = 6, 12, 18 and 24 m. The foundation depth was kept constant at D = 25 m. In a related study, the writers investigated the influence of relative foundation compressibility on performance of reinforced walls having a range of backfill and reinforcement stiffness (**Damians et al. 2014**). In this previous study, the foundation was treated as equivalent linear Winkler springs with stiffness computed as k = E/D where E is the Young's modulus of the foundation soil. In addition, the foundation stiffness varied from k = 4 MPa/m to rigid corresponding to

medium loose sand to intact rock (**Bowles 1996**). In the current study, k = 0.4 to 400 MPa/m corresponding to clay to weathered rock. The lower limit was purposely selected to capture trends in numerical outcomes corresponding to the low end of foundation stiffness. The reinforcement length (L) was taken as 0.7 times the wall height in all cases, and the embedment depth was 0.1×H. These values satisfy minimum criteria in the USA for the wall heights and geometry in this study (**Berg et al. 2009**).

The vertical domain boundaries were fixed in the horizontal direction. The bottom boundary was fixed in both horizontal and vertical directions. The model domain (depth and width) and numerical mesh element refinement were selected to jointly optimize computation time and minimize the influence of problem boundaries. Smaller numerical mesh elements were generated in the soil zone immediately in front of the wall toe and in zones adjacent to all reinforced-soil interfaces and horizontal panel joints. Each numerical wall was built incrementally from the bottom up to simulate construction in the field.

In the sections to follow, the properties of the component materials and their implementation within the PLAXIS program are the same as those reported in the paper by **Damians et al. (2013)**, unless noted otherwise. Hence, some details in the sections to follow are omitted for brevity.

Material Properties and Interfaces

Soil (backfill and foundation): Material properties for the soil zones (backfill and foundation) are summarized in **Table 1**. The soil materials in the majority of simulations are modeled as elastic-plastic materials using the Mohr-Coulomb failure criterion. For simplicity, no attempt has been made to simulate compaction effects during placement of soil layers. The ratio of soil elastic modulus for different soil material zones (e.g., backfill soil and foundation) has been kept constant between matching simulations that vary only with respect to wall height. In this study, the backfill stiffness $E_{(backfill)}$ refers to the soil at 1 m and greater from the back of the concrete panels. At closer distances the soil stiffness is reduced by 50% (**Table 1**). This was done to capture the effect of less compaction energy on soil stiffness using lighter compaction equipment

which is recommended practice immediately behind the wall face to minimize additional compaction-induced loads on the concrete facing panels (**Berg et al. 2009**). The focus of the paper is on the influence of relative compressibility of the joint inclusions, backfill soil zone and foundation soil on wall facing behavior. Hence, a large cohesive strength component (50 kPa) for the foundation soil was adopted to ensure that deformations originating in the foundation soil were within the elastic range of the soil (i.e., working stress conditions) and thereby simplify the interpretation of results

Huang et al. (2009) and **Damians et al. (2014)** demonstrated that the use of more complex non-linear multi-parameter soil constitutive models does not guarantee improved numerical accuracy with measured wall performance. Nevertheless, a number of wall cases were repeated using the hardening soil model that is available in PLAXIS in order examine the sensitivity of numerical outcomes to choice of soil constitutive model for the backfill soil. Hardening model parameters are given in **Table 1**. Details of the model can be found in the PLAXIS software manual (**PLAXIS 2012**). The E_{50}^{ref} value for the hardening soil model was selected to match the elastic modulus of the soil in the corresponding elastic analyses and the same M-C failure criterion was also adopted. The default value of $R_f = 0.9$ in program PLAXIS was used in this study. For project-specific design a lower value may be appropriate (e.g., $R_f = 0.75$) based on fitting to triaxial compression testing of site-specific soils as demonstrated by **Damians et al. (2014)**. However, in the current study the numerical outcomes were found not to be sensitive to the choice of R_f in the range of 0.75 to 0.9 which is likely because the soils remained largely in the working stress (elastic) range. It should be noted that minor soil yielding occurred in a very thin column at the back of the facing, at the foundation toe and at the back of the reinforced soil zone in some simulations with both M-C and hardening soil models. However, large and contiguous soil failure zones in the reinforced soil mass consistent with conventional notions of reinforced soil wall failure did not occur in any simulations.

Facing (concrete panels and bearing pads): The material properties assumed for the precast concrete facing panels and the polymeric bearing pads (horizontal joints) are shown in **Table 2**. The joint axial stiffness was computed based on plan area of each pad, pad modulus and the number of pads per 1.5 m-long panel joint. These calculations result in an initial linear

196 compression response of the joints as a result of the compressive stress-strain behavior of the
197 individual pads (**Figure 3**). The assumption of linear joint stiffness also simplifies parametric
198 analyses to isolate the influence of the compressibility of the horizontal joints between facing
199 panels, wall height and reinforcement layer location on vertical loads transmitted through the
200 wall facing. For walls with a large number of very stiff bearing pads, the assumption of linear
201 compression is reasonable for in-service (operational) conditions. For walls with more
202 compressible joints, the assumption of linear compression is satisfactory if compression is
203 restricted to (say) 10% for HDPE pads and (say) 40% for EPDM pads based on published data
204 (**Neely and Tan 2010; Choufani et al. 2011**). In the simulations to follow, the bearing pads
205 were assumed to have an initial thickness of t = 20 mm (**Table 2**). The minimum available gap
206 space is taken as 20 mm by assuming that the gap at the concrete panel lip(s) is at least equal to
207 20 mm (**Figure 1**).
208
209 *Reinforcement*: The reinforcement layers were placed at uniform vertical spacing of 0.75 m in
210 each wall and each layer was assigned a constant axial stiffness (J) (**Table 3**). The axial stiffness
211 was increased with depth below the top of the wall to capture the increase in number of
212 reinforcing strips in a layer which is common practice for steel strip walls, and/or to capture the
213 increase in total cross-section area per unit running length of wall that is used in some steel
214 ladder wall systems constructed with circular bars. The axial stiffness values vary from about J =
215 30 MN/m to 100 MN/m for wall heights of H = 6 to 24 m, respectively. These values are
216 consistent with the range of values reported by **Bathurst et al. (2011)** for steel grid reinforced
217 soil walls and **Huang et al. (2012)** for steel strip reinforced soil walls.
218
219 *Interfaces*: In the earlier preliminary study by **Damians et al. (2013)**, a sensitivity analysis was
220 carried out using a range of interface friction coefficient R = tan δ / tan ϕ where δ is soil-concrete
221 panel interface friction angle and ϕ is the friction angle of the backfill soil. The best value was
222 determined to be R = 0.3 based on comparison of predicted vertical toe loads with measured
223 results from an instrumented field wall (**Runser et al. 2001; Damians et al. 2014**), and thus is
224 the value used in the current study. The soil-reinforcement interaction was modeled assuming a
225 perfect bond behavior (i.e., R = 1). This value is consistent with measured pullout test data for

ribbed steel strips and well compacted granular soils reported in the literature (**Schlosser and Elias 1978**; **Miyata and Bathurst 2012; Bathurst et al. 2011**).

Results of Analyses

Influence of Joint Stiffness and Soil Stiffness on Vertical Facing Panel Loads

Numerical results using linear axial (compressive) joint stiffness are reported first. **Figure 4** shows load factor (ratio of measured vertical toe load to sum of panel self-weights) plotted against depth of joint below the top of the wall for four different wall heights, two joint materials, and four different combinations of backfill and foundation stiffness. The soil constitutive models are linear elastic with M-C failure criterion in all cases. For reference purposes, the data for cases with H = 18 m are quantitatively similar to previously reported results in the earlier related paper by **Damians et al. (2013)**. Only numerical results in which there was a positive gap are presented. No attempt was made to simulate the concrete-to-concrete contact condition, which in practice should be avoided. The plots also show the load factor at which 10% and 40% compression of the joint is exceeded. These values correspond to the first break point in the compressive stress-strain plots for the HDPE and EPDM bearing pads shown in **Figure 3**. Hence, the plots in **Figure 4** assume that the initial linear elastic behavior of the bearing pads persist at all compressive strains. The grey symbols in the figure identify numerical outcomes where the compression of the bearing pads has extended beyond the initial linear stress-strain region in **Figure 3** but the panels are not in contact.

The influence of the above parameters on load factor magnitude and vertical distribution is complex. The following observations can be made from **Figure 4**:

1. In general, for the same foundation stiffness condition, decreasing the stiffness of the joint material (EPDM versus HDPE in these examples) and/or increasing the stiffness of the backfill soil leads to reduced load factor at similar depths below the top of the wall (compare **Figure 4a** with **4c**, and **Figure 4b** with **4d**).

2. For the case of a relatively less stiff backfill soil ($E_{(backfill)}$ = 10 MPa) (**Figure 4a** and **4b**) there is generally steadily increasing load factor with depth below the wall regardless of joint material.
3. For the relatively stiff backfill condition ($E_{(backfill)}$ = 100 MPa) the vertical load factor is less for the stiffer foundation soil case at similar depths (compare **Figure 4c** with **4d**).
4. For walls with the more compressible joints (EPDM) the vertical load factor becomes more uniform with depth for increasing backfill soil stiffness and the stiff foundation condition with $E_{(foundation)}$ = 1000 MPa (compare **Figure 4b** with **Figure 4d**). The explanation is that the joint stiffness for the EPDM cases in this parametric study is similar in magnitude to the backfill soil. Hence, relative downward movement of the wall facing and backfill soil is less for the case with $E_{(backfill)}$ = 100 MPa.
5. For the case of HDPE joint material and $E_{(backfill)}$ = 100 MPa and $E_{(foundation)}$ = 10 MPa, there is relatively little influence of wall height on the magnitude of load factor (**Figure 4c**).
6. For many cases the linear-elastic region for the HDPE bearing pads is exceeded. The elastic strain limit of the EPDM pads is greater and it is for this reason that numerical outcomes where the elastic limit of the material has not been exceeded are more easily visible in the figure (e.g., **Figures 4c** and **4d**).

Two walls cases with linear elastic HDPE and EPDM bearing pads were repeated using the hardening soil model in PLAXIS for the backfill soil only. This soil model captures non-linear stress-dependent stiffness behavior of frictional soil materials. The results of simulations using both soil models are compared in **Figure 5**. To minimize visual clutter, numerical outcomes with strains greater than the initial elastic limit are not identified. In general, the load factor response curves are similar to those in **Figure 4** but are shifted to the right indicating that qualitative features in **Figure 4** are preserved in **Figure 5**. Hence, the PLAXIS soil hardening model predicts greater vertical load transferred through the facing column than the simpler linear-elastic plastic model. Since the focus of the paper is largely on the relative performance of the walls using a range of assumed wall component material properties and wall heights, the quantitative differences in the response curves in **Figure 5** are judged not to be a practical concern from a performance point of view.

However, it is worth noting that the run times were up to six times longer for numerical simulations using the hardening soil model compared to matching cases using the simpler soil model. For example, using a desk top computer with an Intel© Core 2 Duo Pa8600 (2.40 GHz) (Intel, Santa Clara, California) central processor, the computer solved wall models with H = 24 m in approximately 20 min for elastic M-C soil model cases and 120 min for the hardening soil model cases. The numerical results presented hereafter are for simulations carried out using linear elastic M-C soil models.

Influence of Joint Stiffness and Soil Stiffness on Panel-Joint Gap

Figure 6 shows the vertical load factor generated at selected joint locations (depth z) for each wall height (H) case versus relative joint stiffness. Relative joint stiffness is calculated as the ratio of the product of the pad elastic modulus, pad area and number of pads per joint, to the product of backfill soil stiffness and joint (pad) thickness. In this study t = 20 mm which is a typical thickness for these pads (**Damians et al. 2013**). As a useful reference, the relative joint stiffness data points in **Figure 6** are matched to the number of bearing pads manufactured from HDPE and EPDM materials per 1.5 m-long joint. The plots show that the load factor tends to one as the stiffness ratio goes to zero (e.g., as axial bearing pad stiffness goes to zero). For relative joint stiffness values greater than about one the load factor is reasonably constant at each depth location. A load factor of one is possible (i.e., no downdrag forces) if the compressibility of the horizontal joint is sufficient to allow the concrete panels to settle with the backfill soil.

Figure 7 shows the computed joint gap thickness (at the location of the bearing pads) and axial (compressive) strain at three normalized depth locations. Three different numbers of EPDM and HDPE pads per panel joint (2, 4 and 6) were assumed in these calculations. The plots show that the magnitude of backfill stiffness plays a major role in joint compression. For the same fixed relative joint stiffness value, the gap compression is less for the stiffer backfill soil condition and gap closure increases with depth below the top of the wall. The influence of foundation stiffness is less for cases with relative joint stiffness of (say) 0.5 or greater. Some additional numerical results are shown for the case of an intermediate value of backfill stiffness ($E_{(backfill)}$ = 50 MPa).

317 An alternative presentation of the results of parametric analyses is given in **Figure 8**. Here
318 isolines of equal gap thickness are plotted for each wall height scenario and different
319 combinations of backfill and foundation stiffness, and different numbers of EPDM and HDPE
320 bearing pads. These plots can be used for design to select the minimum number of 20 mm-thick
321 pads at each horizontal joint location to not exceed a specified minimum gap thickness. The 12
322 mm- and 5 mm-gap isolines in the figure may be taken as the range of minimum acceptable post-
323 construction values based on recommendations by **Berg et al. (2009)** and **BSI BS8006 (2010)**,
324 respectively, and observations by **Choufani et al. (2011)**.
325
326 ***Influence of Joint Stiffness and Soil Stiffness on Vertical Facing Settlement***
327
328 **Figure 9** shows computed settlements at the top of the concrete facing for different wall heights
329 and combinations of other parameter values. Previous figures demonstrate that the magnitude of
330 load factor is sensitive to joint compressibility and relatively less sensitive to foundation
331 stiffness. However, the plots in **Figure 9** show that foundation compressibility is much more
332 important than joint compressibility when settlement of the wall facing (or backfill) is a concern.
333 Examples when wall settlements are important are where the wall supports or adjoins other
334 structures.
335
336 ***Influence of Bearing Pad Constitutive Model on Gap Thickness Prediction***
337
338 A linear compression law for the joint bearing pads has been adopted in the current study and in
339 the earlier related paper by **Damians et al. (2013)**. A linear model has the advantage of
340 simplicity which facilitates comparison and understanding of the contribution of the many
341 factors that influence vertical load transmission and horizontal panel joint compression in steel
342 reinforced soil walls. Linear models are satisfactory for very stiff horizontal joints (e.g., large
343 numbers of bearing pads are used at each joint) and/or the strains are kept within elastic limits
344 (about 10% for HDPE and 40% for EPDM type). However, the actual compression behavior of
345 individual HPDE bearing pads of typical thickness (t = 20 mm) taken to large strains is
346 sigmoidal shaped. For 20 mm-thick bearing pads manufactured from EPDM, the compression
347 behavior at large strains is better captured by a bilinear stress-strain hardening model (**Figure 3**).

348

349 **Figure 10** reproduces results of numerical calculations similar to those in **Figure 7** but adopting
350 the bilinear (EPDM) and trilinear (HDPE) compressive stress-strain approximations to the
351 measured data in **Figure 3**. Comparison of **Figure 10** with **Figure 7** shows that in many cases
352 the gap thicknesses using the linear compressive stress-strain model are similar or smaller.
353 Hence, using the simpler linear model will give similar or more conservative (safer) design
354 outcomes. The exceptions are some scenarios with 2 or 4 HDPE bearing pads in combination
355 with relative joint stiffness values greater than about 0.5 and 5, and relatively stiff and soft
356 backfill soil cases, respectively. However, for these cases simply increasing the number of HDPE
357 pads per joint to 6 pieces will return the joint compression response to the initial linear behavior
358 and thus the two figures will give the same predictions.

359

360 ## Conclusions

361

362 The concrete panels that form the facing of steel reinforced soil walls must carry loads that are
363 greater than the self-weight of the panels. The vertical load carried by the facing will result in
364 compression of the horizontal joints between adjoining panels. Excessive vertical loads and/or
365 excessively compliant bearing pads can lead to panel to panel contact which can cause the
366 concrete panels to crack or spall.

367

368 This paper extends the work of **Damians et al. (2013**) by quantitatively investigating the
369 influence of wall height, backfill soil constitutive model and bearing pad compression model on
370 numerical predictions of vertical panel loads and gap compression. Rather than attempt to
371 associate a particular value of elastic modulus with a particular soil type, which is problematic
372 for frictional soils, a wide range of soil stiffness values spanning two orders of magnitude was
373 used to capture the possible influence of foundation modulus on wall facing response. The
374 numerical results show that the backfill soil stiffness, foundation compressibility and horizontal
375 joint stiffness all influence the magnitude and distribution of vertical load through the height of
376 the wall and bearing pad compression. The current study demonstrates that qualitative trends in
377 vertical load factor are preserved when a more advanced stress-dependent stiffness soil
378 hardening model is used for the backfill soil compared to the simpler linear-elastic Mohr-

379 Coulomb model. There are detectable higher vertical loads through the concrete facing panels
380 and more gap compression in some cases using the advanced backfill soil model, but the
381 differences are small and thus judged not to be of practical concern.
382
383 Despite the influence of many factors on the magnitude of vertical facing load and joint
384 compression, a set of design charts was developed that can be used to select the number and type
385 of bearing pads placed at the horizontal joints between the concrete panels so that gap closure is
386 restricted to tolerable amounts and vertical loads transmitted through the concrete panels are not
387 excessive. Additional analysis results are presented as design charts that can be used to estimate
388 the settlement at the top of the concrete facing units. These charts demonstrate that settlement of
389 the concrete facing is most sensitive to the compressibility of the foundation soil.
390
391 An important caveat to the results presented here is that only vertical facing loads and uniform
392 joint compression are considered. In actual walls there is also the possibility of differential
393 settlements along horizontal joints and panel tilting. These deformations can also lead to panel
394 contact and subsequent cracking and spalling. Numerical modelling of the type used in this
395 investigation is not a practical approach to investigate these potential but infrequent modes of
396 failure. Rather, these types of problems are best prevented through good construction quality
397 control including careful initial alignment of the bottom row of panels on a level and well-
398 supported footing.
399
400

401 ## Acknowledgments

402

403 The authors wish to acknowledge the support of the Universitat Politècnica de Catalunya-
404 BarcelonaTech (UPC) and the funding received through the research projects BIA2010-20789-
405 C04-01 from the Ministry of Education and Innovation and CTM2013-47067-C2-1-R from the
406 Ministry of Economy and Competitiveness of Spain.

407

408

409 **REFERENCES**

410

411 American Association of State Highway and Transportation Officials (AASHTO) (2014). LRFD
412 Bridge Design Specifications. 7th edition, Washington, DC, USA.

413

414 Bathurst, R.J., Huang, B. and Allen, T.M. (2011). Load and resistance factor design (LRFD)
415 calibration for steel grid reinforced soil walls. Georisk, 5(3-4): 218-228.

416

417 Berg, R.R., Christopher, B.R. and Samtani, N.C. (2009). Design and construction of
418 mechanically stabilized earth walls and reinforced soil slopes, Vol. I. National Highway Institute,
419 Federal Highway Administration, U.S. Department of Transportation, Washington, DC.

420

421 Bowles, J.E. (1996). Foundation analysis and design. 5th Ed., McGraw Hill, New York.

422

423 BSI (British Standards Institution). (2010). Code of Practice for Strengthened/Reinforced Soil
424 and Other Fills. BSI, Milton Keynes, UK, BS 8006.

425

426 Choufani, C., Wu, P., Gagnon, G. and Macintosh, M. (2011). A precast faced mechanical
427 stabilized earth solution for a 20 metre high mining crusher wall with various technical and site
428 challenges. In CD proceedings of 2011 Pan-Am Canadian Geotechnical Conference, Toronto,
429 Canada, Paper 625, 6 p.

430

431 Damians, I.P., Bathurst, R.J., Josa, A., Lloret, A. and Albuquerque, P.J.R. (2013). Vertical facing
432 loads in steel reinforced soil walls. ASCE Journal of Geotechnical and Geoenvironmental
433 Engineering, 139(9): 1419-1432.

434

435 Damians, I.P., Bathurst, R.J., Josa, A. and Lloret, A. (2014). Numerical study of the influence of
436 foundation compressibility and reinforcement stiffness on the behavior of reinforced soil walls.
437 International Journal of Geotechnical Engineering, 8(3): 247-259.

438

439 Damians, I.P., Bathurst, R.J., Josa, A. and Lloret, A. (2015). Numerical analysis of an
440 instrumented steel-reinforced soil wall. ASCE International Journal of Geomechanics, 15(1):
441 04014037.
442
443 Findlay, T.W. (1978). Performance of a reinforced earth structure at Granton. Ground
444 Engineering, 2(7): 42-44.
445
446 Gerber, T.M. (2012). Assessing the Long-Term Performance of Mechanically Stabilized Earth
447 Walls. (National Cooperative Highway Research Program (NCHRP) Synthesis 437).
448 Transportation Research Board, Washington, DC.
449
450 Huang, B., Bathurst, R.J. and Allen, T.M. (2012). Load and resistance factor design (LRFD)
451 calibration for steel strip reinforced soil walls. ASCE Journal of Geotechnical and
452 Geoenvironmental Engineering, 138(8): 922-933.
453
454 Huang, B., Bathurst, R.J. and Hatami, K. (2009). Numerical study of reinforced soil segmental
455 walls using three different constitutive soil models. ASCE Journal of Geotechnical and
456 Geoenvironmental Engineering, 135(10): 1486-1498.
457
458 Miyata, Y. and Bathurst, R.J. (2012). Analysis and calibration of default steel strip pullout
459 models used in Japan. Soils and Foundations, 52(3): 481-497.
460
461 Neely, W.J. and Tan, S.L. (2010). Effects of second order design factors on the behavior of MSE
462 walls. Earth Retention Conference 3. Earth Retaining Structures Committee of the Geo-Institute
463 of ASCE. Geotechnical Special Publications (GSP) n. 208. In Proceedings of the 2010 Earth
464 Retention Conference held in Bellevue, Washington, August 1-4, 2010, pp. 522-530.
465
466 PLAXIS (2008). Reference Manual, 2D - Version 9.02. PLAXIS B.V., Delft University of
467 Technology, Netherlands (http://www.plaxis.nl/).
468
469 PLAXIS (2012). Material models manual, Plaxis. Delft Univ. of Technology, Delft, Netherlands.

Runser, D.J., Fox, P.J. and Bourdeau, P.L. (2001). Field performance of a 17 m-high reinforced soil retaining wall. Geosynthetics International, 8(5): 367-391.

Schlosser, F. and Elias, V. (1978). Friction in reinforced earth. In Proceedings of ASCE Symposium on Earth Reinforcement, Pittsburgh, PA, USA, pp. 735-763.

Yu, Y., Bathurst, R.J. and Miyata, Y. (2015a). Numerical analysis of a mechanically stabilized earth wall reinforced with steel strips. Soils and Foundations 55(3): 536–547.

Yu, Y., Damians, I.P. and Bathurst, R.J. (2015b). Influence of choice of FLAC and PLAXIS interface models on reinforced soil-structure interactions. Computers and Geotechnics, 65:164-174.

Table 1. Soil properties.

Parameters	Backfill		Foundation
Unit weight (kN/m^3)	19		18
Cohesion (kPa) [1]	5 [2]		50
Friction angle, ϕ (degrees)	36[3]		30
Dilatancy angle, ψ (degrees) [4]	6		0
Elastic Mohr-Coulomb soil model:	< 1.0 m from facing [5]	> 1.0 m from facing	
Elastic modulus (MPa)	- soft case: 5 - stiff case: 50	- soft case: 10 - stiff case: 100	- soft case: 10 - stiff case: 1000
Poisson's ratio (-)	0.3		0.3
Hardening soil model: [6]	($m = 0.5$ and $R_f = 0.9$) [7]		
E_{50}^{ref} (MPa) [8]	- soft case: 5 - stiff case: 50	- soft case: 10 - stiff case: 100	n/a
Poisson's ratio (-)	0.2		n/a

[1] Soils are assumed as no-tension materials (tension cut-off).

[2] Non-zero cohesion value has been assumed for the numerical model to ensure numerical stability at very low confining pressure.

[3] Peak plane strain friction angle of granular soil is greater than the corresponding triaxial or direct shear test values. Hence, value of ϕ = 36 degrees used in simulations is in agreement with conventional triaxial compression or direct shear peak friction angles of (say) 30 to 34 degrees. The latter are minimum recommended friction angles for select granular fills in North American practice (**Berg et al. 2009**).

[4] Assumed as $\psi = \phi - 30^o$.

[5] Area where less compaction energy is used during construction to minimize lateral loads on facing panels. The elastic stiffness modulus was assumed to be 50% of the elastic stiffness modulus of the well-compacted soil for both linear elastic Mohr-Coulomb and hardening soil model cases.

[6] Dilatancy and dilation angle are included in hardening model.

[7] $m = 0.5$ is the power term for stress-level dependency of soil stiffness and the value used here is typical for sand soils. R_f corresponds to the failure ratio between the ultimate deviatoric stress and the asymptotic value of the shear strength.

[8] E_{50}^{ref} corresponds to the reference confining stress-dependent stiffness modulus for primary triaxial loading, corresponding to the secant stiffness at a deviatoric stress level equal to half the failure stress. Reference confining stress = 100 kPa. The unloading and reloading stiffness modulus (E_{ur}^{ref}) was assumed to be 3 times higher than E_{50}^{ref} which is the default assumption in the PLAXIS manual. The tangent stiffness for primary oedometer loading (E_{oed}^{ref}) was assumed to be equal to E_{50}^{ref}.

Table 2. Concrete panel and bearing pad (joint) properties.

		Bearing pads [1]					
		EPDM [2]			HDPE [3]		
		number of pads per panel joint					
Parameters	Panels	2	4	6	2	4	6
Axial stiffness, J = EA (kN/m)	5600×10^3	130	260	390	1100	2200	3300
Bending stiffness, EI ($kN/m^2/m$)	9150	0.25	0.50	0.75	2.10	4.20	6.20
Poisson's ratio	0.15		0.49			0.40	

[1] assuming a pad plan dimension area of 0.008 m^2 for both material cases, and a panel width 1.5 m in the running length direction of the wall and pad thickness of t = 20 mm.

[2] EPDM = ethylene propylene diene monomer.

[3] HDPE = high-density polyethylene.

519

520 **Table 3.** Reinforcement layer stiffness.

Wall height, H (m)	Reinforcement layer location, depth from top of wall, z (m)	Linear-elastic stiffness, $J_{(reinforcement)} = (EA)_{reinforcement}$ (MN/m)
6	0.4 to 5.3	28.1
12	0.4 to 6.4	28.1
	7.1 to 8.6	37.5
	9.4 to 10.9	46.9
	11.6	56.3
18	0.4 to 7.1	29.3
	7.9 to 11.6	44.0
	12.4 to 14.6	58.6
	15.4 to 17.6	73.3
24	0.4 to 7.1	29.3
	7.9 to 11.6	44.0
	12.4 to 15.4	58.6
	16.1 to 19.1	73.3
	19.9 to 22.9	87.9
	23.6	102.6

521

522 Notes: E = elastic modulus of steel = 200 GPa; A = cross-section area of steel strip or bars.

523

524

525 **Figure 1.** Vertical load in concrete panel wall face and gap compression. Note: Some panel
526 systems have a lip at the back and front of the panel joint.
527
528 **Figure 2.** Finite element model geometry.
529
530 **Figure 3**. Horizontal joint compressive stress-strain behavior of EPDM and HDPE pad materials.
531 Note: EPDM = ethylene propylene diene monomer; HDPE = high-density polyethylene.
532
533 **Figure 4**. Vertical load factor versus joint depth for different wall height (H) and backfill-
534 foundation stiffness combinations, and assuming two 20 mm-thick bearing pads (EPDM or
535 HDPE) per 1.5 m-long joint with linear axial (compressive) stiffness. Note: Numerical results
536 using linear elastic M-C soil model.
537
538 **Figure 5**. Comparison of numerical results using PLAXIS hardening soil model and linear
539 elastic M-C soil model for backfill soil. Vertical load factor versus joint depth for different wall
540 height (H) and backfill-foundation stiffness combinations, and assuming two 20 mm-thick
541 bearing pads (EPDM or HDPE) per 1.5 m-long joint with linear axial (compressive) stiffness.
542
543 **Figure 6**. Load factor versus relative joint stiffness. Note: Parameter z is depth of horizontal
544 joint from top of wall.
545

546 **Figure 7**. Joint gap thickness and compression (at location of bearing pads) versus relative joint
547 stiffness for different normalized depths of joint below top of wall (z/H) using linear bearing pad
548 compressive stress-strain models.
549
550 **Figure 8**. Isolines of joint vertical gap thickness for different wall height H, joint stiffness
551 (different numbers of bearing pads per joint), and different backfill soil and foundation stiffness
552 conditions. Wall heights: H = 6 m (a), H = 12 m (b), H = 18 m (c), and H = 24 m (d).
553
554 **Figure 9.** Influence of wall height, soil backfill and foundation stiffness, bearing pad type and
555 number on settlement at the top of the concrete panel facing.
556
557 **Figure 10**. Joint gap thickness and compression versus relative joint stiffness for different
558 normalized depths of joint below top of wall (z/H) using bilinear (EPDM) and trilinear (HDPE)
559 bearing pad compressive stress-strain models.
560

561

562

563

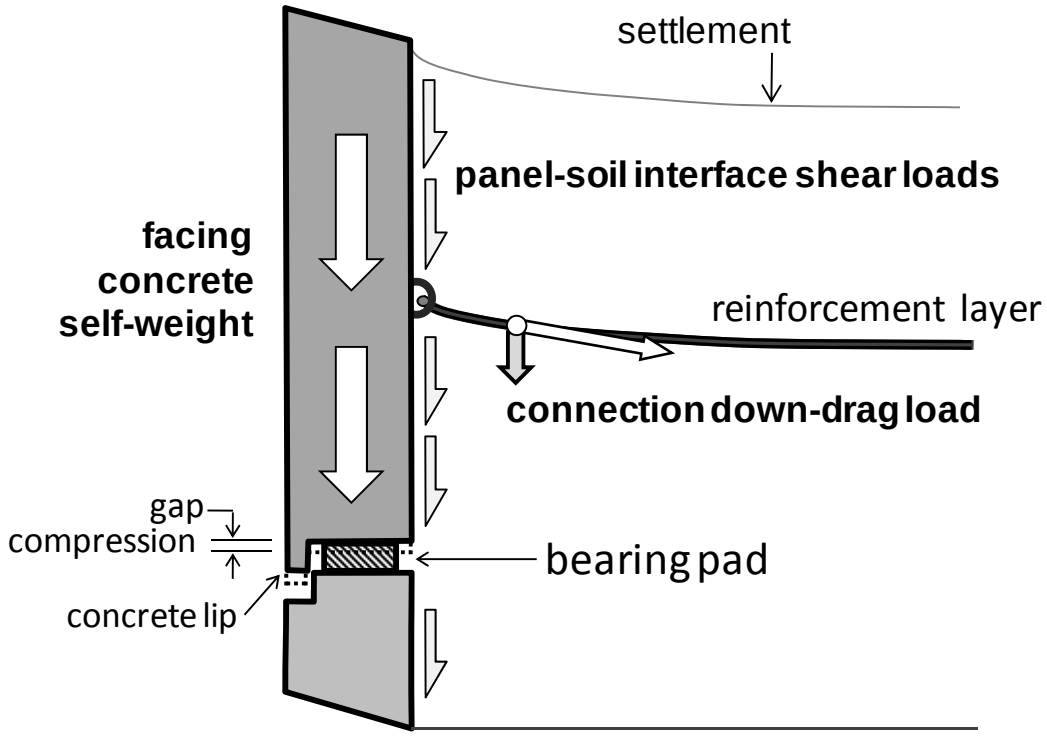

564

565

566 **Figure 1.** Vertical load in concrete panel wall face and gap compression. Note: Some panel
567 systems have a lip at the back and front of the panel joint.

568

569

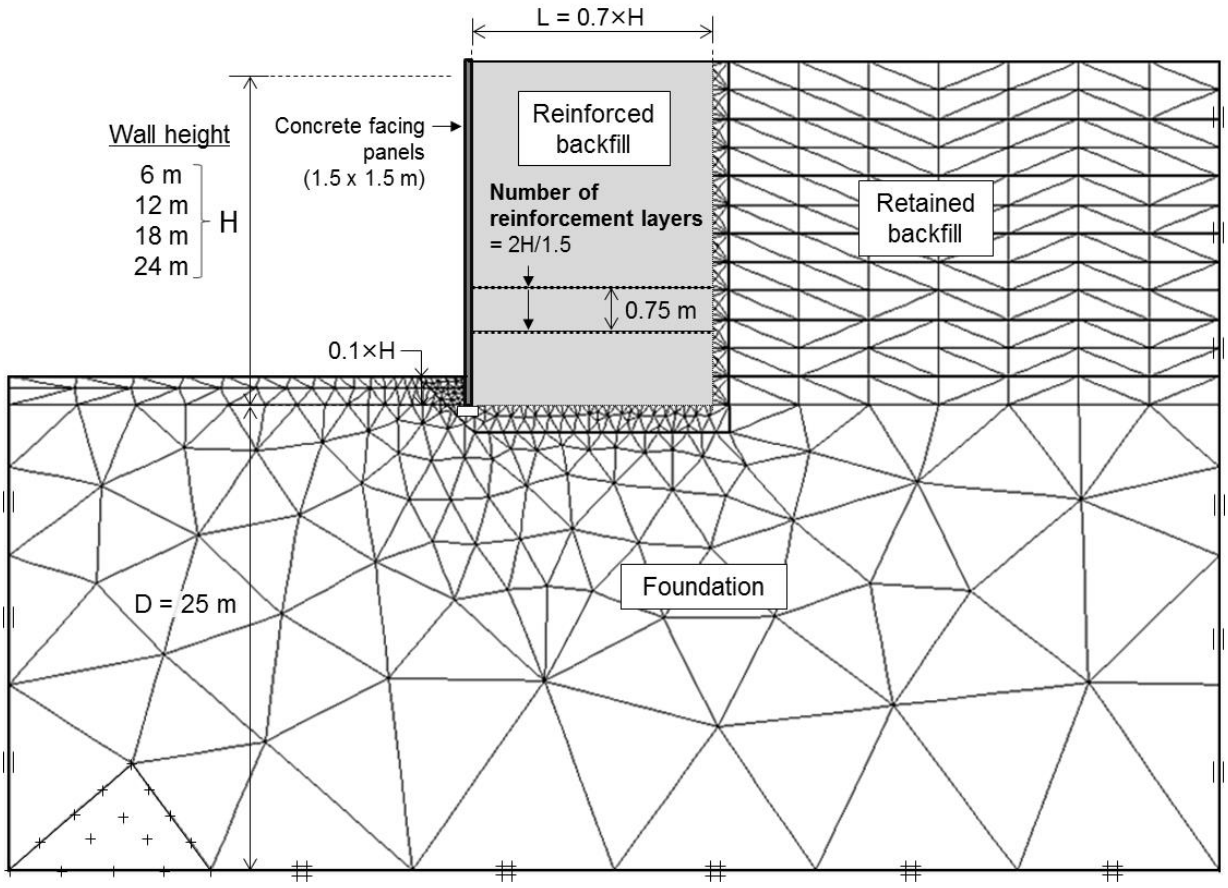

570

571

572 **Figure 2.** Finite element model geometry.

573

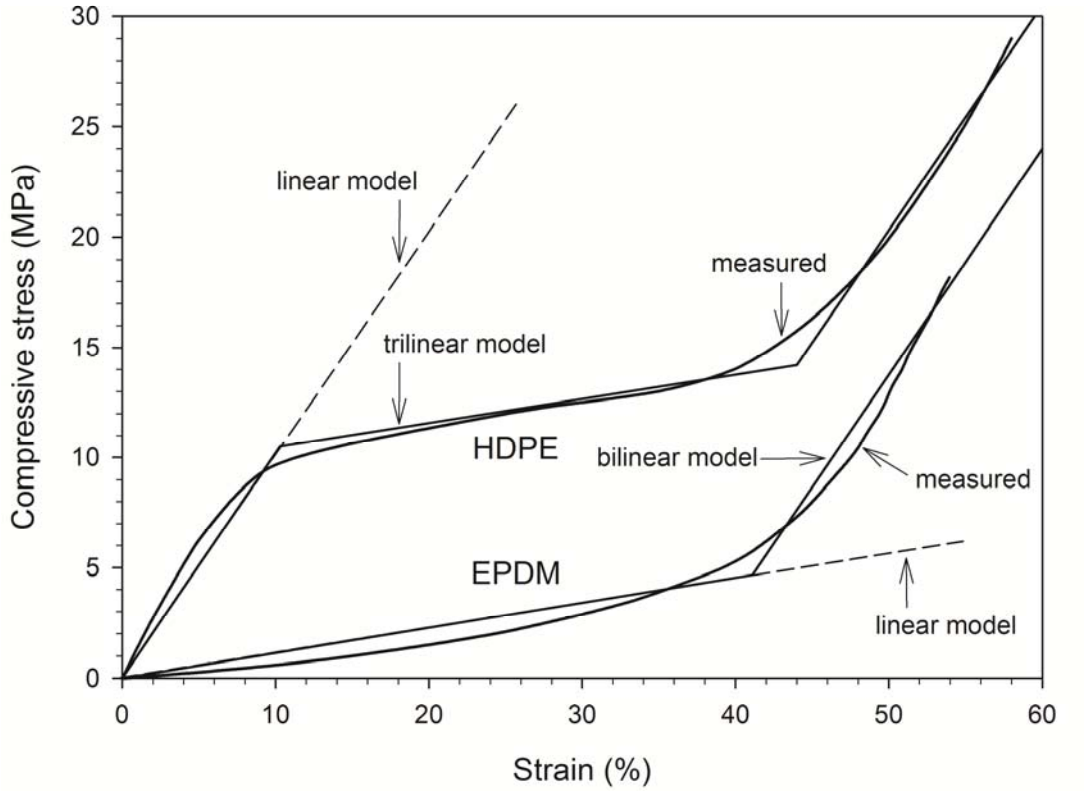

574
575

576 **Figure 3**. Horizontal joint compressive stress-strain behavior of EPDM and HDPE pad materials.

577 Note: EPDM = ethylene propylene diene monomer; HDPE = high-density polyethylene.

578
579
580

581

582

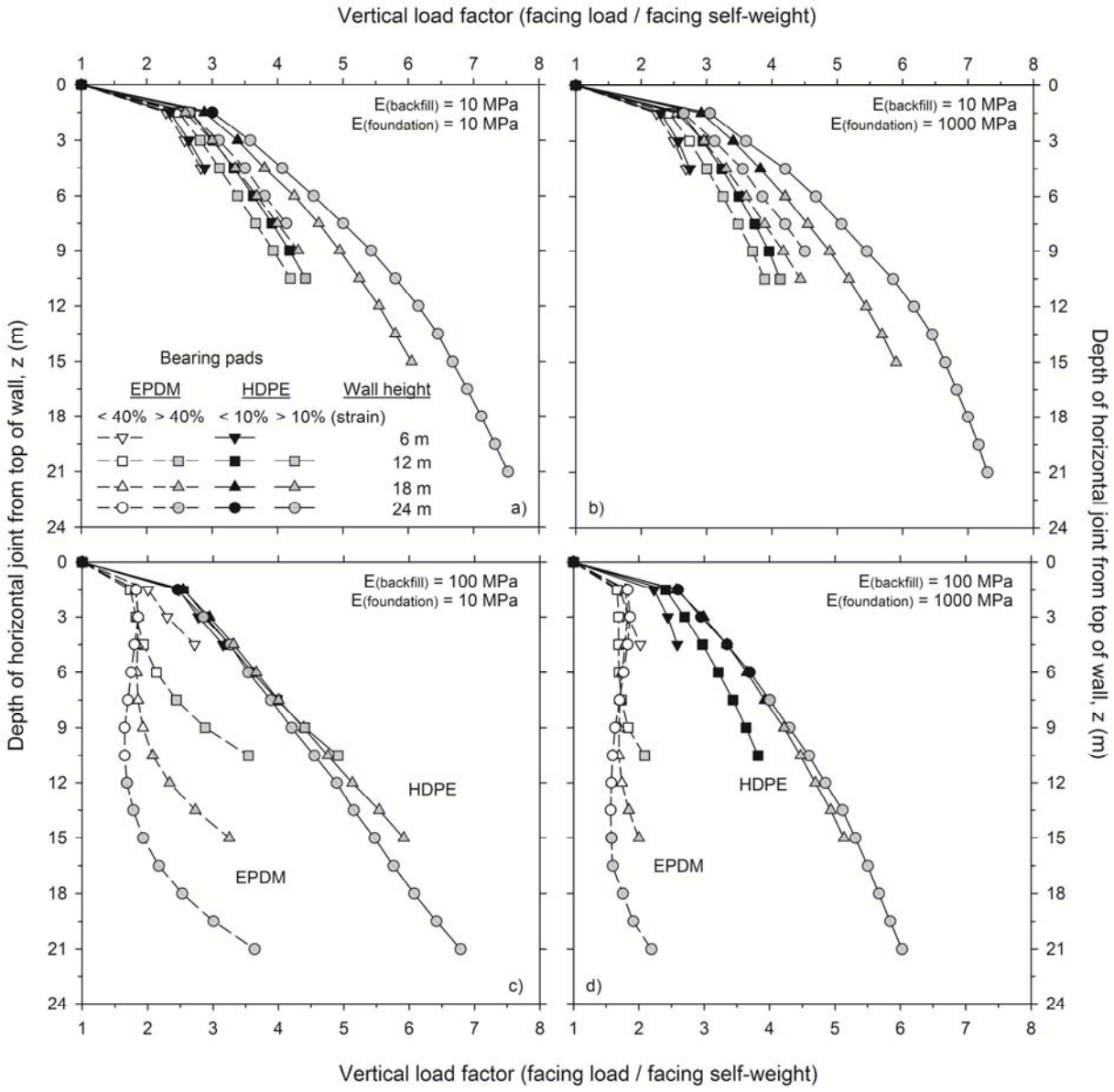

583

584

585 **Figure 4**. Vertical load factor versus joint depth for different wall height (H) and backfill-
586 foundation stiffness combinations, and assuming two 20 mm-thick bearing pads (EPDM or
587 HDPE) per 1.5 m-long joint with linear axial (compressive) stiffness. Note: Numerical results
588 using linear elastic M-C soil model.

589

590

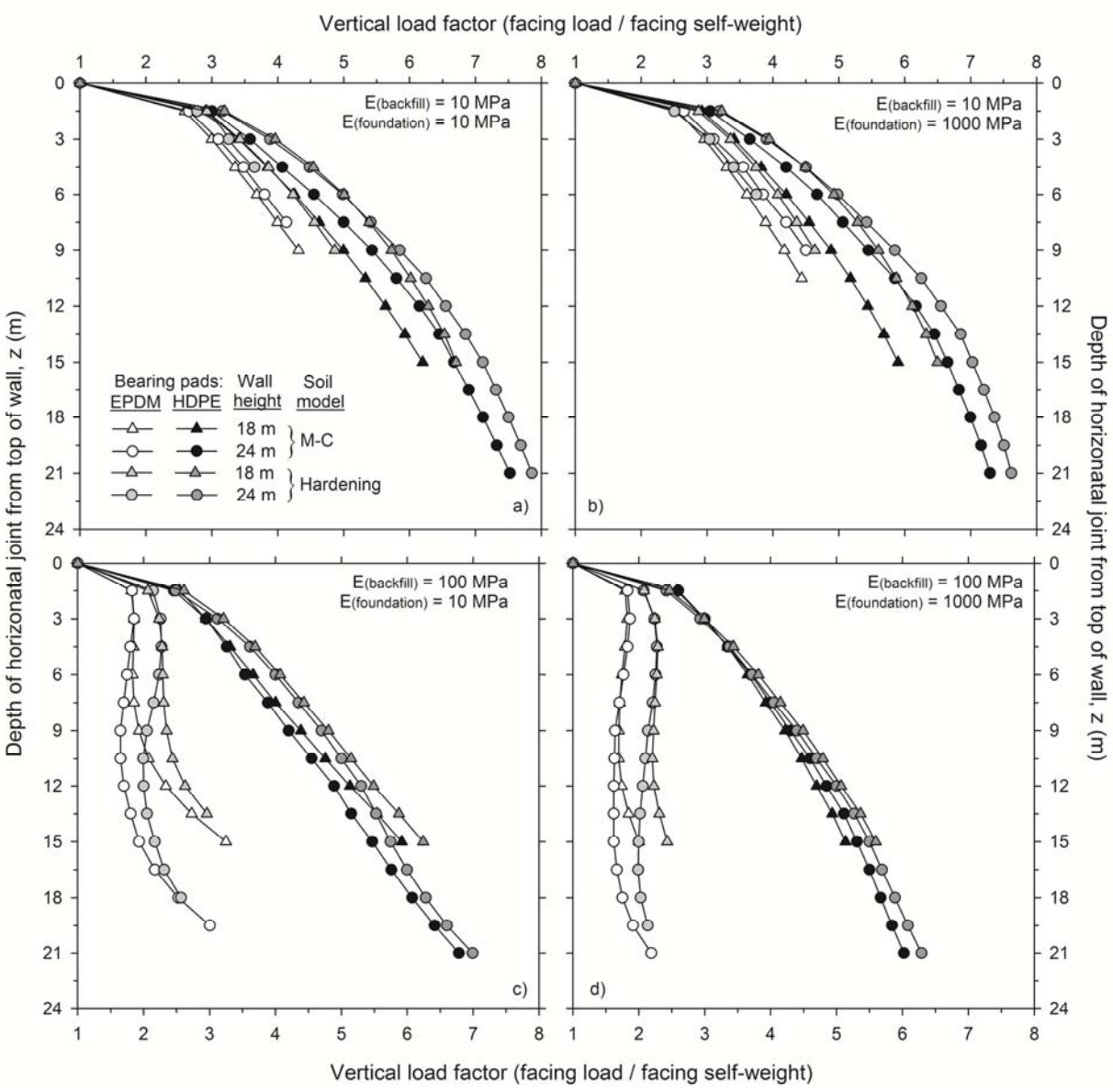

591

592

593 **Figure 5**. Comparison of numerical results using PLAXIS hardening soil model and linear
594 elastic M-C soil model for backfill soil. Vertical load factor versus joint depth for different wall
595 height (H) and backfill-foundation stiffness combinations, and assuming two 20 mm-thick
596 bearing pads (EPDM or HDPE) per 1.5 m-long joint with linear axial (compressive) stiffness.

597

598

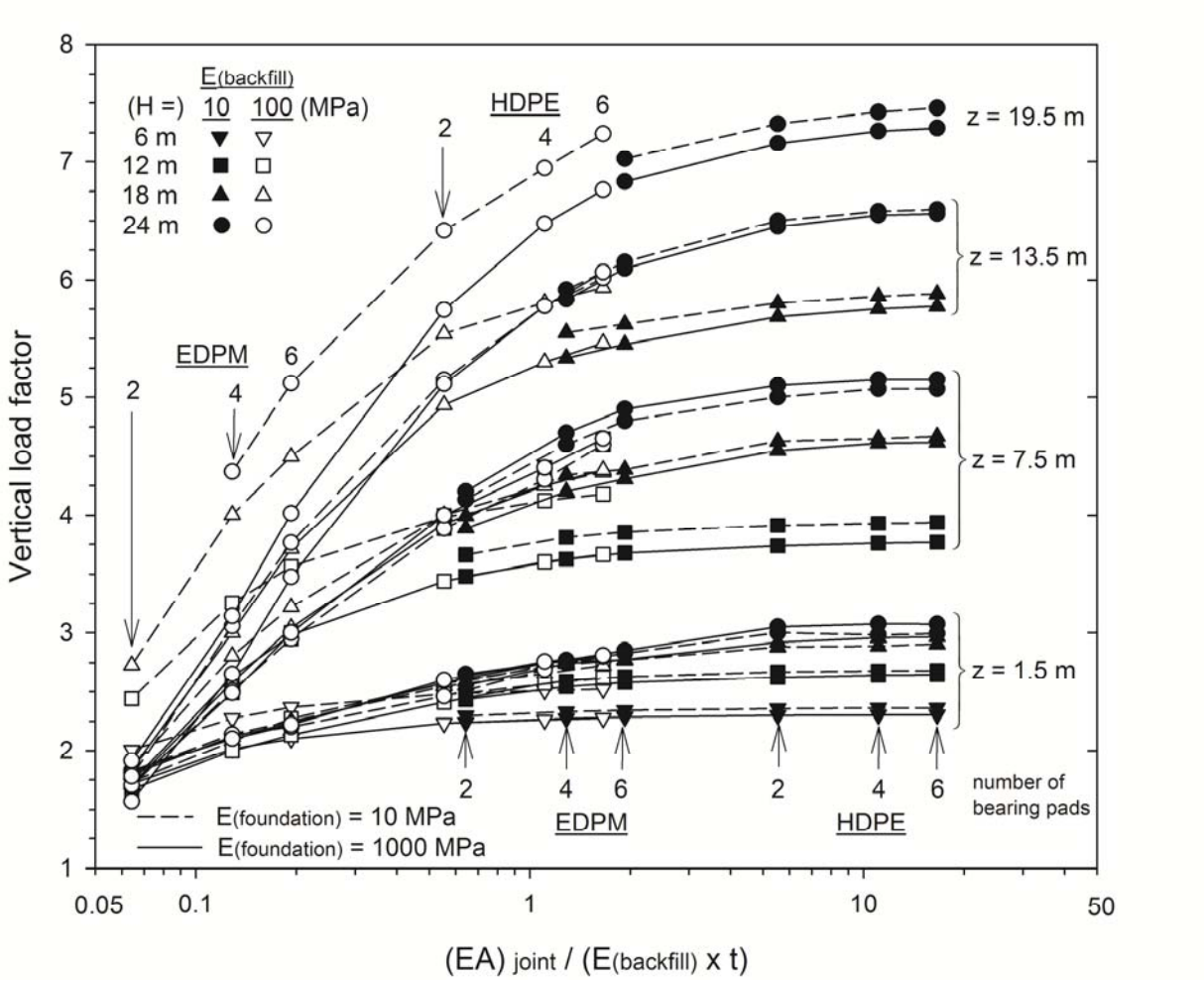

Figure 6. Load factor versus relative joint stiffness. Note: Parameter z is depth of horizontal joint from top of wall.

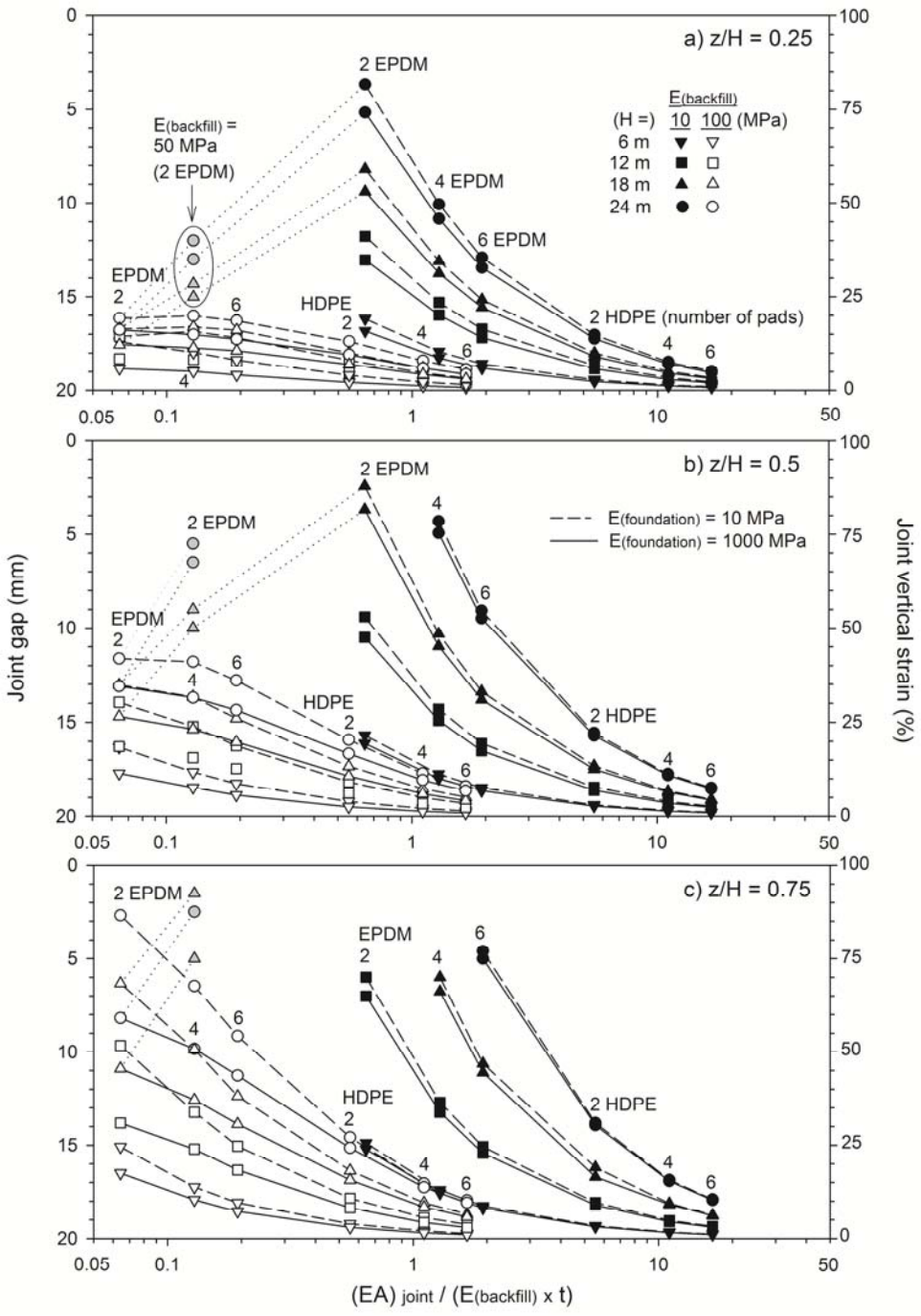

604

605 **Figure 7**. Joint gap thickness and compression (at location of bearing pads) versus relative joint
606 stiffness for different normalized depths of joint below top of wall (z/H) using linear bearing pad
607 compressive stress-strain models.

608 a) H = 6 m

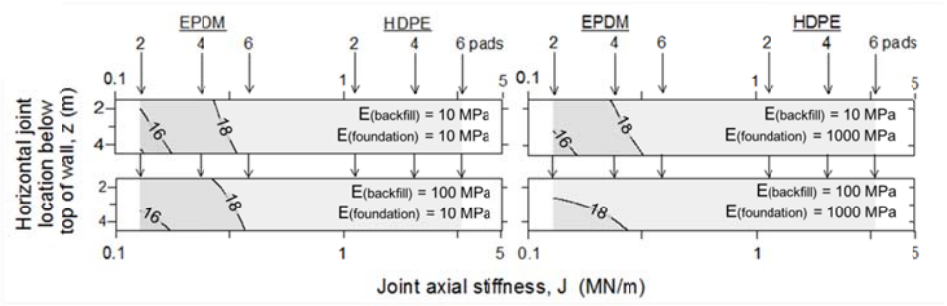

609
610
611
612
613
614

615 b) H = 12 m

616

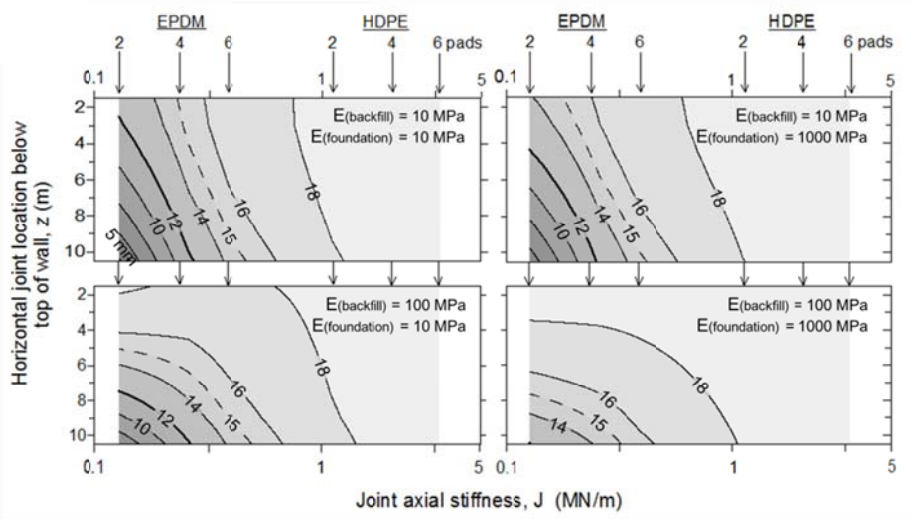

617

618 c) H = 18 m

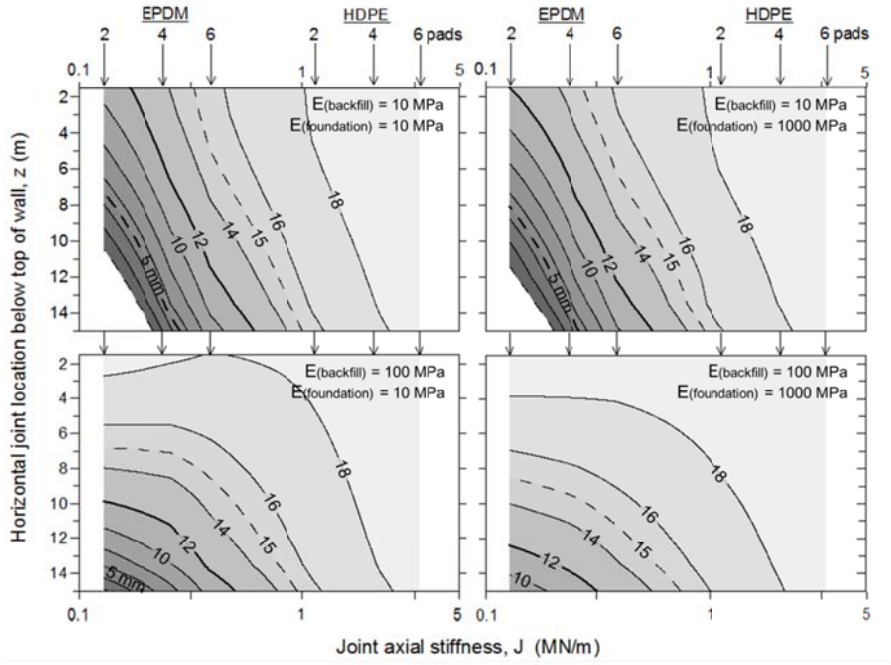

619
620

d) H = 24 m

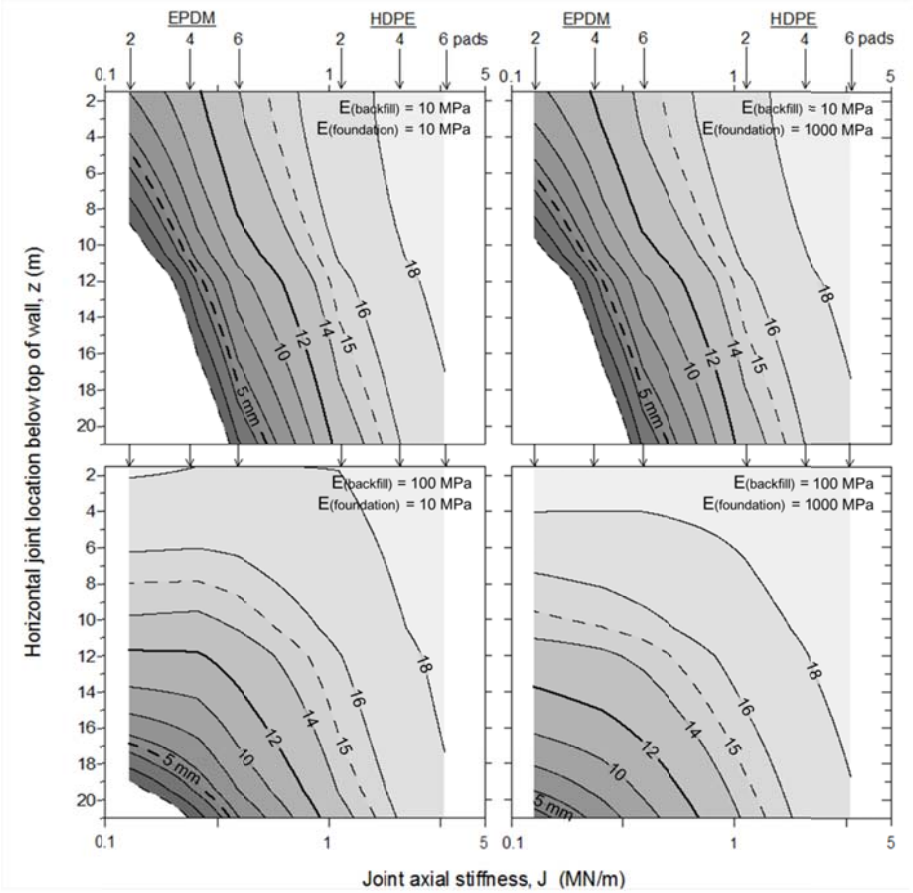

Figure 8. Isolines of joint vertical gap thickness for different wall height H, joint stiffness (different numbers of bearing pads per joint), and different backfill soil and foundation stiffness conditions. Wall heights: H = 6 m (a), H = 12 m (b), H = 18 m (c), and H = 24 m (d).

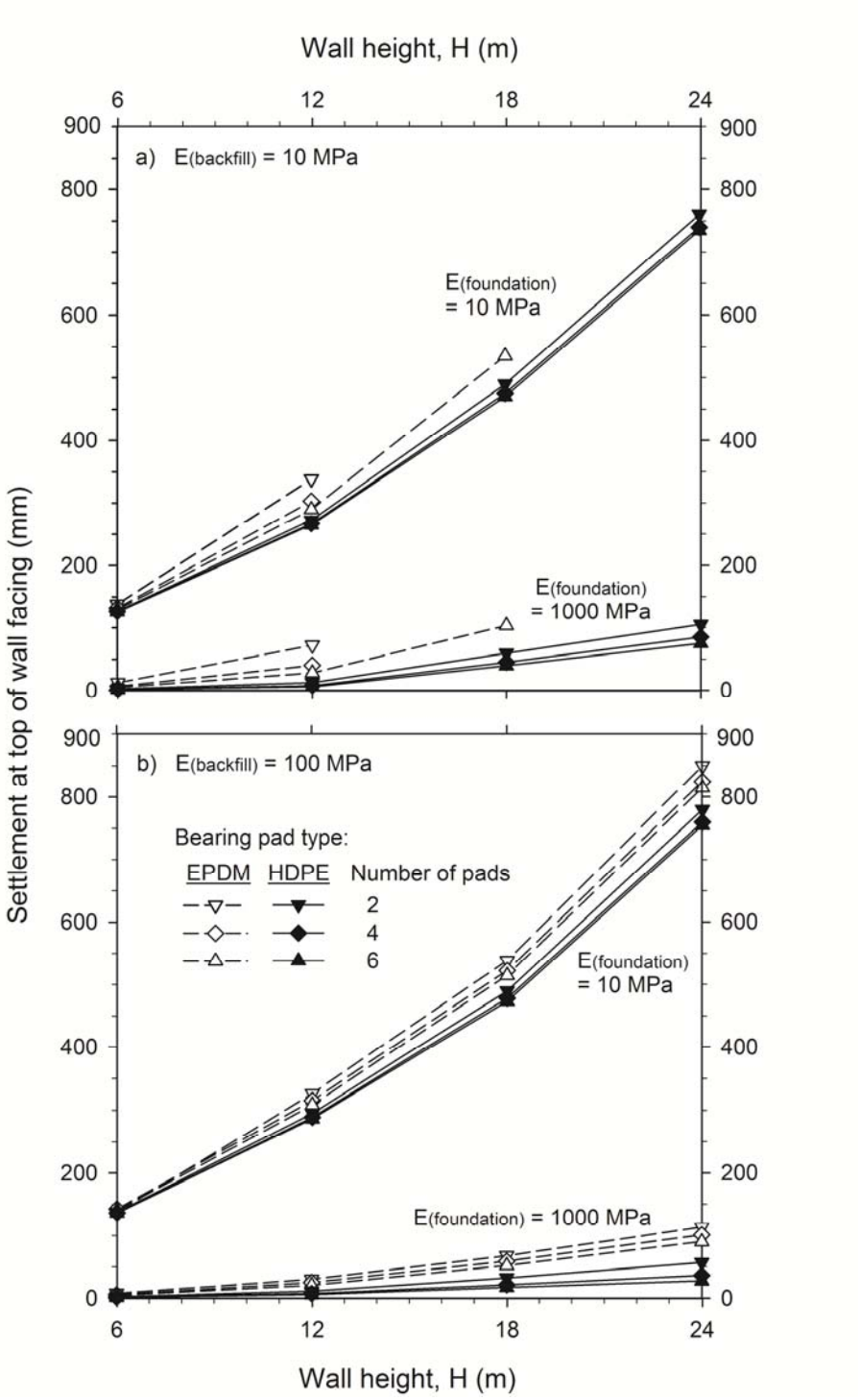

Figure 9. Influence of wall height, soil backfill and foundation stiffness, bearing pad type and number on settlement at the top of the concrete panel facing.

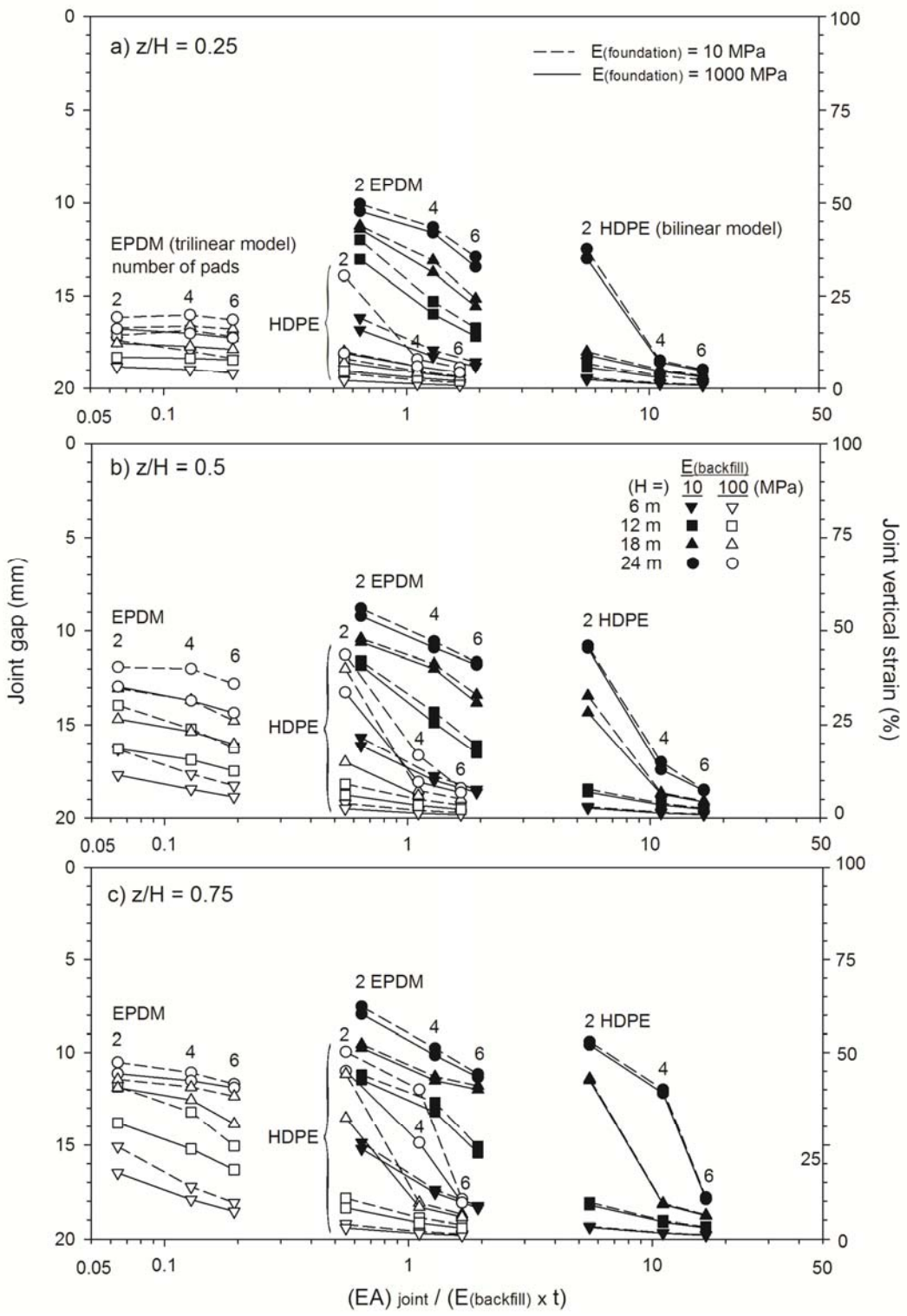

Figure 10. Joint gap thickness and compression versus relative joint stiffness for different normalized depths of joint below top of wall (z/H) using bilinear (EPDM) and trilinear (HDPE) bearing pad compressive stress-strain models.